Do turbulent premixed flame fronts in spark-ignition engines behave like passive surfaces?

Gülder, Ömer L.; Smallwood, Gregory J.

Publisher's version / Version de l'éditeur:
https://doi.org/10.4271/2000-01-1942
Combustion in Diesel and SI Engines, SAE Special Publication; Volume SAE/SP-00/1549, 2000

MARIA CLANCY
DGO
INST FOR CHEM PROCESS & ENVIR TECH
NATIONAL RESEARCH COUNCIL CANADA
M-12, ROOM 141, 1200 MONTREAL RD.
OTTAWA, ON K1A 0R6
CANADA

SAE TECHNICAL
PAPER SERIES

2000-01-1942

Do Turbulent Premixed Flame Fronts in Spark-Ignition Engines Behave Like Passive Surfaces?

Ömer L. Gülder and Gregory J. Smallwood
Combustion Research Group, National Research Council Canada

Reprinted From: Combustion in Diesel and SI Engines
(SP–1549)

CEC

and

SAE The Engineering Society For Advancing Mobility Land Sea Air and Space®
INTERNATIONAL

International Spring Fuels & Lubricants
Meeting & Exposition
Paris, France
June 19-22, 2000

ISSN 0148-7191

2000-01-1942

Do Turbulent Premixed Flame Fronts in Spark- Ignition Engines Behave Like Passive Surfaces?

Ömer L. Gülder and Gregory J. Smallwood
Combustion Research Group, National Research Council Canada

ABSTRACT

A widely held belief in the combustion community is that the chemical and hydrodynamic structure of a stretched laminar premixed flame can be preserved in a turbulent flow field over a range of conditions collectively known as the flamelet regime, and the homogeneous charge spark-ignition engine combustion falls within the domain of this regime. The major assumption in the laminar flamelet concept as applied to the turbulent premixed flames is that the flame front behaves as a constant-property passive scalar surface, and an increase in the wrinkled flame surface area with increasing turbulence intensity is the dominant mechanism for the observed flame velocity enhancement. The two approaches that have been recently used for estimating a measure of the wrinkled flame surface area in spark-ignition engines and other premixed flames are the flame surface density concept and fractal geometry. A critical assessment of the experimental fractal parameters reported in literature indicated that these are not capable of correctly predicting the turbulent burning velocity using the available fractal area closure model. A similar conclusion has been reached after examining the surface density data from flames of different geometries including spark-ignition engine flame fronts. The assumption made in fractal and surface density approaches that the turbulent flame front is a passive scalar surface can not be justified, and the applicability of the flamelet approach may be limited to a much smaller range of conditions than presently believed.

INTRODUCTION AND BACKGROUND

The structure and velocity of flame fronts in homogeneous charge spark-ignition engines have been the subjects of several experimental and theoretical research efforts. This continuing interest is mainly due to the fact that the answer may have significant impacts in areas of practical importance. The combustion process in spark-ignition engines takes place in a turbulent environment. For the disc shaped combustion chamber the turbulence is mostly generated by the high shear flows during the induction process and modified during the compression. It is well established that the turbulence intensity as well as the mean flow increases almost in a linear fashion with increasing engine speed [1].

The turbulence decays rapidly towards the end of the induction process and the characteristic dissipation time for the turbulent kinetic energy is smaller than the engine time scales [1]. The turbulence during the induction exhibits a strong anisotropy, and the turbulence intensity as well as the mean velocity shows significant spatial variations. For disc shaped chambers, the turbulence when averaged over several cycles, displays a homogeneous and more isotropic structure towards the end of the compression stroke for both swirling and non-swirling flows [1-3].

The combustion engine community is widely subscribed to the belief that the turbulent flame in practical homogeneous charge SI engines is a wrinkled laminar flame. There seems to be strong experimental evidence for existence of this type of flame structure. In an experiment using molecular Rayleigh scattering, it was concluded that the turbulent flame front is made up of wrinkled laminar flames and it may include occasional islands of unburned mixture [4]. Similar observations were reported by Keck [5] and Abraham et al. [6].

Turbulent premixed flame propagation was first investigated by Damköhler [7] who pointed to two limiting cases based on the magnitude of the scale of turbulence as compared to the flame front thickness. For low-intensity, large-scale turbulence, Damköhler proposed that S_T/S_L, the ratio of the turbulent burning velocity (S_T) to the laminar burning velocity (S_L), is proportional to A_u/A_o, the ratio of the wrinkled flame surface area (A_u) to the flow cross section area (A_o). For high-intensity, small-scale turbulence, combustion takes place in a distributed manner rather than a front propagation. The identification of the turbulent premixed combustion regimes (i.e., two limiting cases of Damköhler and the regime(s) in between the two) in general, and the limits of the wrinkled flame regime in particular have been an integral part of the turbulent premixed flame propagation issue [8-13].

The wrinkled flame regime mainly covers the conditions where the chemistry is fast in turbulent premixed combustion. Fast chemistry criterion is based on a Damköhler number, Da, which is defined as a ratio of the turbulent time, τ_T, to the laminar flame time, τ_F, i.e.,

$$\mathrm{Da} = \frac{\tau_T}{\tau_F} = \frac{\Lambda S_L}{\delta_L u'} \qquad (1)$$

where Λ is the turbulence integral length scale, u' is the turbulent velocity fluctuation, and δ_L is the laminar flame front thickness. The wrinkled flame regime exists where $\mathrm{Da} > 1$ and the Karlovitz number, Ka, is less than about unity. Karlovitz number is defined as the ratio of the laminar flame time, τ_F, to the Kolmogorov time scale, τ_η,

$$\mathrm{Ka} = \frac{\tau_F}{\tau_\eta} = \left(\frac{\delta_L}{\eta}\right)^2 \qquad (2)$$

where η is the Kolmogorov length scale. The turbulent Reynolds number is defined as the ratio of turbulent diffusivity to laminar diffusivity, i.e.

$$\mathrm{Re}_\Lambda = \frac{u'\Lambda}{\nu} = \frac{\Lambda u'}{\delta_L S_L} \qquad (3)$$

where ν is the kinematic viscosity.

On a plot of Damköhler number, Eq.1, versus turbulent Reynolds number, it is possible to identify the approximate region of wrinkled flames. Such a plot is shown in Figure 1 [6]. Also shown in Figure 1 is the estimated range of engine combustion conditions. In the reaction sheet regime it is assumed that the propagating flame fronts are wrinkled and convoluted by the turbulence.

The attempts to quantify the effects of turbulence on premixed turbulent burning velocity, in the reaction sheet regime, have encountered several challenges, both theoretically and experimentally. Substantial progress has been made in the development of numerical codes to simulate the 3D unsteady flow structures in SI engines. However, progress has been slower in simulating the combustion process due to a lack of a robust and computationally effective prediction model for turbulent premixed flame propagation [14]. The concept of laminar flamelets provides a useful tool to describe the turbulent premixed flames using simple but reasonable assumptions to overcome some of the challenges posed by the problem [15]. This concept assumes that the combustion within a turbulent flame is confined to asymptotically thin moving laminar flamelets which are embedded in the turbulent flow [15,16]. Since the instantaneous behaviour of these thin layers is the same as those of laminar flames, the turbulent burning velocity can be approximated by the product of the flamelets' surface area and the laminar burning velocity corrected for the effect of stretch and flame curvature [17]. Most recent experimental and numerical work also implies that the wrinkled flame regime (where the flamelet approach can be used) is much wider than previously thought [18-21].

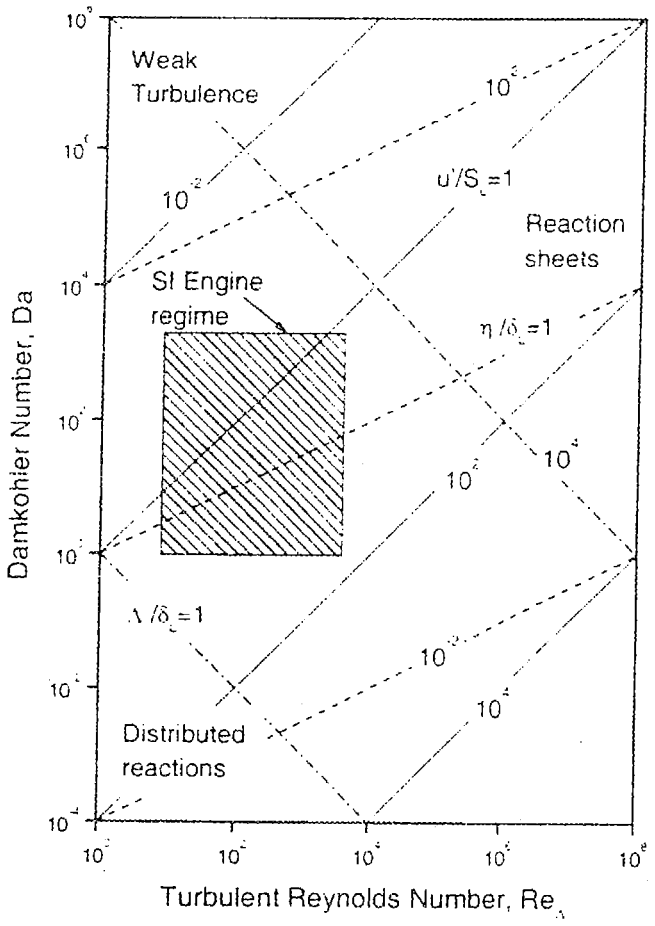

Figure 1. Approximate regimes of turbulent premixed combustion in Damköhler vs turbulent Reynolds number space. The rectangle is an estimate of the regimes applicable to spark ignition engine combustion. Adapted from Ref.6.

The simulation efforts of spark-ignition engines include a number of approaches and most of them are based on the flamelet concept. The flamelet concept is implemented in simulations either through a fractal closure model, see e.g. [22], or through the flame surface density formulation [22-26].

The present work briefly reviews the fractal and flame surface density approaches, and critically assesses the experimental fractal and flame surface density data from premixed flames of different geometries and SI engines flame fronts reported in literature. The implications of this assessment are discussed.

FRACTAL DESCRIPTION OF FLAMELETS

FRACTAL CLOSURE FOR TURBULENT FLAMES

One way of measuring the area of a three dimensional surface is to count the number of cubic boxes, $N(\varepsilon)$, of size ε required to cover the whole surface. The area then is of order $N(\varepsilon)\varepsilon$. If the surface is a classical one, i.e., can be described by Euclidean geometry, $N(\varepsilon)$ approaches to

a constant value independent of ε. For a fractal surface, which exhibits self-similarity over a wide range of scales, the measured area estimates will increase with increasing resolution (i.e. decreasing value of ε) according to the power law [27]. The variation of the area with the resolution ε for a fractal surface, on a log-log scale, exhibits a straight line with the slope $(2 - D)$, where D is the fractal dimension of the surface. Therefore, the area $A(\varepsilon)$ is given by

$$A(\varepsilon) \propto \varepsilon^{(2-D)} \tag{4}$$

The range of scales over which the power laws of the type Eq.4 holds is bounded by cutoffs on both ends imposed by physical limits.

As originally suggested by Damköhler [7], the ratio of the turbulent to laminar flame velocity should be proportional to the ratio of the instantaneous flame surface area of the turbulent flame, A_t, to the flow cross section area, A_o, i.e,

$$\frac{S_T}{S_L} \approx \frac{A_t}{A_o} \tag{5}$$

Then, the fractal geometry yields the following relationship [28]

$$\frac{S_T}{S_L} = A \left(\frac{\varepsilon_o}{\varepsilon_i} \right)^{D-2} \tag{6}$$

where ε_o is the outer cutoff, ε_i is the inner cutoff, and A is a constant of order one.

Applying fractal geometry concepts to the description of the wrinkled flame front surfaces has been shown to provide reasonable estimates of the turbulent flame velocity for the assumed values of the cutoff scales and the fractal dimension [28,29]. Gouldin et al. [30] and Gouldin and Miles [31] have proposed closure models based on a fractal representation of flamelets in turbulent premixed flames. It is assumed that the flamelet surface density may be represented by a fractal surface of dimension D for a range of length scales between the inner cutoff ε_i and the outer cutoff ε_o. Refinements to the closure model [30] and the flame speed model [28] are presented in [32]. It is argued that the prefactor A in Eq.6 is a variable with a laminar limit of 1 and an intense turbulence limit of 2, but may not be bounded between 1 and 2. Also, in the presence of large scale doubling back of the wrinkled surface, the fractal area expression in Eq.6 may require modification by adding a second variable, a multiplying factor to account for doubling back. The success and the applicability of these models are dependent on the availability of reliable fractal dimension, and inner and outer cutoff information.

The inner cutoff represents the smallest scale for the interaction of turbulent eddies with the premixed flame front. When the eddies are smaller than the inner cutoff, the flame crosses an eddy before the eddy evolves significantly, so the flowfield is effectively stationary from the viewpoint of flame propagation [33]. Direct numerical simulation of turbulent premixed flames [18] and the experimental work on interaction of vortices with flame fronts [19,34] confirm the existence of a physical lower cutoff scale. The outer cutoff, in a very general sense, can be defined as the size of the experiment. In turbulent flows, it has been proposed that the outer cutoff is comparable to the integral length scale of turbulence.

FRACTAL CHARACTERISTICS OF FLAME FRONTS

The most widely used method to estimate the fractal dimension and cutoffs of the turbulent flame fronts is flame tomography. The flame fronts are usually visualized by seeding the reactant flow with submicron oil droplets and illuminating the droplets with a sheet of laser radiation. The oil droplets evaporate rapidly at the flame front, causing a sharp decrease in Mie scattered radiation, which indicates the transition from unburned to burned gases [35]. Alternately, planar laser induced fluorescence of a combustion produced species can be used to mark the instantaneous flame front location. One of the popular and relatively easy to implement methods is the planar laser induced fluorescence of OH [36]. Mantzaras et al. [37,38] and Yoshiyama et al. [39] used sub-micron TiO_2 seeding particles to mark the shape and location of the flame front in optically accessed spark ignition engine combustion chambers, relying on rapid expansion in the burned gases to disperse the particles and cause a decrease in scattered radiation.

For turbulent premixed flames, Gouldin [28] used a fractal dimension of 2.37 in his formulation, whereas Gülder [29] used 7/3, as inferred by Kerstein [33]. The fractal dimension, D, of premixed turbulent flames has been measured by several investigators [37-42] and a correlation giving fractal dimension as a function of nondimensional turbulent velocity fluctuation, u'/S_L (ratio of turbulent velocity fluctuation to the laminar burning velocity), has been proposed [41]. This correlation and the experimental data presented in the cited literature assert that the fractal dimension D approaches the fractal dimension of nonreacting turbulent flows 2.37 as u'/S_L increases. Most recent studies [35,43,44], on the other hand, have been unable to confirm the results of the previous work. The maximum fractal dimension measured (average of several flame images) was 2.21 for u'/S_L =15 in a Bunsen flame [44] and 2.23 for u'/S_L =8.6 in a V-flame [43].

A comparison of all available experimental data on fractal dimension of turbulent premixed flame fronts has been made in Fig.2. The difference between previous measurements and data coming from present authors' group is significant for $u'/S_L > 1$. The data of [37,38,41,42] show a fractal dimension about 2.33-2.37 when $u'/S_L \geq 3$, whereas Gülder et al. [44] indicate a value about 2.2 for nondimensional turbulence intensities between 0.9 and 15.

DISCUSSION OF THE FRACTAL RESULTS

The difference observed in Fig.2 between the experimental data sets of fractal dimension is significant for nondimensional turbulence intensities larger than unity. How

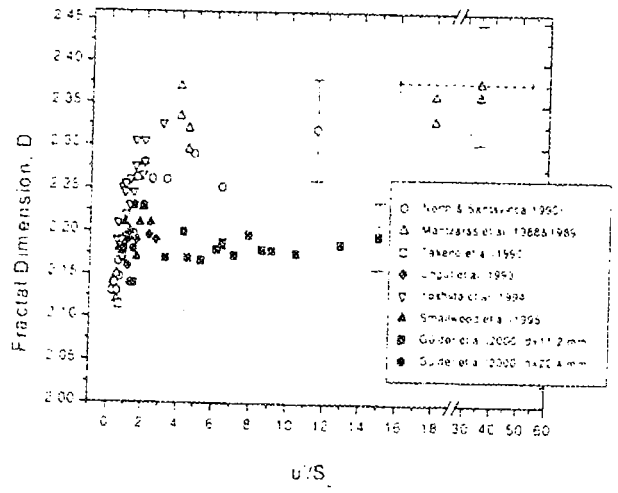

Figure 2. Comparison of the experimental fractal dimension data from different studies [44]. For clarity typical error bars are shown for highest turbulence intensity points only. The horizontal error bar of the data point of [37, 38] indicates the range of u'/S_L in the engine combustion chamber during the experiment. Note the axis break and the scale change on x-axis.

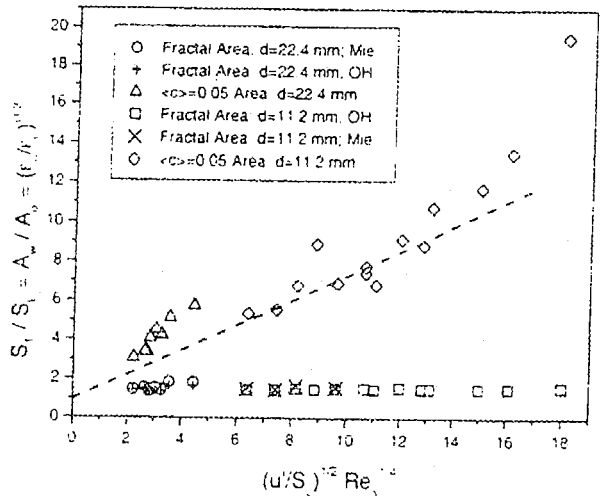

Figure 3. Turbulent burning velocity as determined by fractal and nonfractal methods [44]. For the nonfractal method, the ratio of the area of an equivalent laminar cone ($A_L = Q/S_L$, where Q is the volume flow rate of the premixed reactants) to the area marked by the $< c >=0.05$ was used. Area marked by the $< c >=0.05$ denotes the lower bound of the flame brush. The straight dashed line is the prediction of Eq.7. d is the diameter of the burner, and OH and Mie represent the imaging methods.

can this discrepancy between the data of [35,43,44] and the results of the other investigators [37,38,41,42] be explained? This issue has been addressed in [44], and it has been shown that the culprit for the difference seen in Fig.2 is due to the fractal image analysis method. It has also been demonstrated with examples that the correct fractal dimension of turbulent premixed flame fronts is about 2.2 and it is not sensitive to turbulence intensity.

Experimental observations on turbulent premixed flames have shown that S_T/S_L increases with increasing turbulence. So the term $(\varepsilon_o/\varepsilon_i)^{D-2}$ is expected to increase with increasing u'/S_L in accordance with Eqs. 5 and 6. Figure 3, taken from Ref.44, shows the variation of fractal area, $A(\varepsilon_o/\varepsilon_i)^{D-2}$, as function of $(u'/S_L)^{1/2}Re_\Lambda^{1/4}$ assuming A =1. Also shown in Fig.3 is the estimated turbulent burning velocities from reactant flow rates and the cone area of the averaged flame images at $< c >=0.05$. The fractal area shows no evidence of dependence on the approach flow turbulence. The straight dashed line indicates the model proposed in [29]

$$S_T/S_L = 1 + 0.63(u'/S_L)^{1/2}Re_\Lambda^{1/4} \qquad (7)$$

which agrees with the estimated S_T/S_L from the reactant flow velocity and the flame cone area.

It was proposed that scales smaller than the laminar flame thickness affect the turbulent flame propagation [45], and it was reported that a proper fractal modelling of turbulent burning velocities should consider both fractal and nonfractal (area increase due to scales smaller than the inner cutoff) contributions [46]. Smallwood et al. [35], however, has shown that the inclusion of area increase due to wrinkling scales smaller than the inner cutoff has little effect on the fractal prediction of the turbulent burning velocity.

Several turbulent flame propagation formulations, including those based on fractal concepts, are founded on the fundamental assumption that S_T/S_L is proportional to the ratio of the wrinkled flame surface area, A_u, to the flow cross section area, A_o, i.e., $S_T/S_L = A_u/A_o$ [7]. If the fractal geometry approach, i.e.

$$A_u/A_o = A(\varepsilon_o/\varepsilon_i)^{D-2} \qquad (8)$$

is yielding a true measure of the wrinkled surface area of the flame front, then $S_T/S_L = A_u/A_o$ may not be a reasonable assumption for the turbulent premixed flames in the flamelet regime. Experimental fractal parameters, i.e., fractal dimension, and inner and outer cutoffs, reported in literature are not capable of correctly predicting the observed turbulent premixed burning velocity. This implies that the other mechanism(s) have nontrivial contributions to the flame propagation in addition to the flame surface area increase by turbulence. Under such circumstances, it would not be possible to describe the flame front propagation in spark-ignition engine combustion by fractal approaches, and the assumption that the turbulent flame front is a passive scalar surface can not be justified. One caveat is that the fractal area expression could be viewed as incomplete in reference to the discussion regarding the prefactor A in Eq.6, and the need for an additional multiplier to include the effect of doubling back of the wrinkled surfaces. Then, more research is needed to resolve the form of the closure model for the fractal area expression.

FLAME SURFACE DENSITY

FLAME SURFACE DENSITY CONCEPT

Within the laminar flamelets regime, the complex chemical kinetics mechanism is represented in terms of the laminar flame propagation speed, S_l. The wrinkling of the flame front surface by turbulence is described by the mean flame-surface area per unit volume which is known as flame surface density, $\Sigma(x)$. The mean rate of conversion of reactants into products per unit volume, $< \dot{w} >$, can be expressed as

$$< \dot{w} > (x) = \rho_r S_L^o I_o \Sigma(x) \qquad (9)$$

where ρ_r is the density of reactants, S_l^o is the unstretched laminar burning velocity, I_o is a factor accounting for the stretch effects, and Σ is the flame surface density. The factor I_o is dependent on the distribution of curvature and strain rates over the flamelet surface. Curvature and strain modify the flamelet structure and result in flame stretch, $\dot{S}$, which can be quantified as

$$\dot{S} = \left(\frac{1}{A} \frac{dA}{d\tau} \right)_F \qquad (10)$$

where A is the area of an element of the flame surface and τ is the time. If $\dot{S}$ is small enough, then a linear analysis shows that [47]

$$S_L = S_L^o - M_a \delta_L^o \dot{S} \qquad (11)$$

Here M_a is the Markstein number and δ_L^o is the laminar flame thickness (unstretched). The ratio $I_o = S_L / S_L^o$ is a matter of much debate in the current turbulent premixed combustion literature (see, e.g. [48]), and the magnitude of I_o inferred from measurements and numerical simulations varies significantly. Some of the approaches assume that for flames with Lewis numbers close to unity, S_L remains close to the laminar flame velocity S_L^o [52], and I_o does not deviate significantly from unity.

Simple algebraic closure models have been proposed for flame surface density, Σ, [49,50]. The Bray-Moss-Libby model [49,50] for Σ is based on the spatial distribution of flame crossings along a contour of the mean progress variable $< c >$, which is 0 in the reactants and 1 in the products, and is given by

$$\Sigma = \frac{g < c > (1 - < c >)}{\sigma_y L_y} \qquad (12)$$

in which g is a constant of the order unity; σ_y is a mean direction cosine; and L_y is a characteristic length related to flame wrinkling.

An alternative formulation for modeling the spatial variation of the flame surface density, based on the gradient of the progress variable across the flame front [51], is

$$\Sigma \equiv < \Sigma' > = < |\nabla c| \delta(c - c_f) > \qquad (13)$$

where ∇c is the spatial flame front gradient, $\delta(c - c_f)$ is the instantaneous flame front position, and Σ' is the instantaneous flame surface density.

Gouldin et al. [30] have proposed a closure model for Σ in terms of fractal parameters for turbulent premixed flames:

$$\Sigma = A (\varepsilon_o / \varepsilon_1)^{D-2} < c > (1 - < c >) / \delta_T \qquad (14)$$

where A is a model constant, $< c >$ is the mean progress variable, and δ_T is the turbulent flame brush thickness.

In equations above, the mean rate of reaction, $< \dot{w} >$, and the flame surface density, Σ, both vary with position; they are mean local variables. An overall reaction rate can be defined by space-averaging Eq.9 over a volume, V, that occupies the reaction zone [52]:

$$\overline{< \dot{w} >} = \frac{1}{V} \int < \dot{w} > (x) dV = \rho_u S_L^o I_o \overline{\Sigma} \qquad (15)$$

where $\overline{\Sigma}(t)$ is defined as:

$$\overline{\Sigma} = \frac{1}{V} \int \Sigma(x) dV = \frac{< A_u >}{V} \qquad (16)$$

in which $< A_u >$ is the total flame surface area within volume, V. From Eq.16, $< A_u >$ is equal to the volume integral of the flame surface density. Then, in view of Eqs.5 and 16, the turbulent flame velocity, S_T, in terms of $< A_u >$ is:

$$S_T = S_L^o I_o \frac{< A_u >}{A_o} = S_L^o I_o \frac{\overline{\Sigma} \cdot V}{A_o} \qquad (17)$$

It should be noted that the volume V encloses the turbulent flame brush.

In flamelet models, the flame surface density is obtained either using an algebraic closure, Eqs.12-14, or by way of a modelled transport equation, known as the Σ-equation. The Σ-equation was first formulated for a turbulent diffusion flame under the name coherent flame model by Marble and Broadwell [53]. In a turbulent flow field, the averaged Σ-equation contains terms representing transport by mean flow, transport by turbulence and flame propagation, and production and destruction by flame stretch of the flame surface. Modelling assumptions are needed for transport due to flame propagation, the turbulent diffusion velocity, and turbulent flame stretch. Unfortunately, these terms are not experimentally accessible. Further discussion on the Σ-equation and its numerical solution schemes can be found in [51,54,55].

To determine Σ for a three-dimensional flowfield from two-dimensional images, knowledge of the orientation of the normal to the flame front relative to the image plane is required. To ascertain the orientation, images from orthogonal planes may be used to determine the mean crossing angle along the line of intersection of the planes.

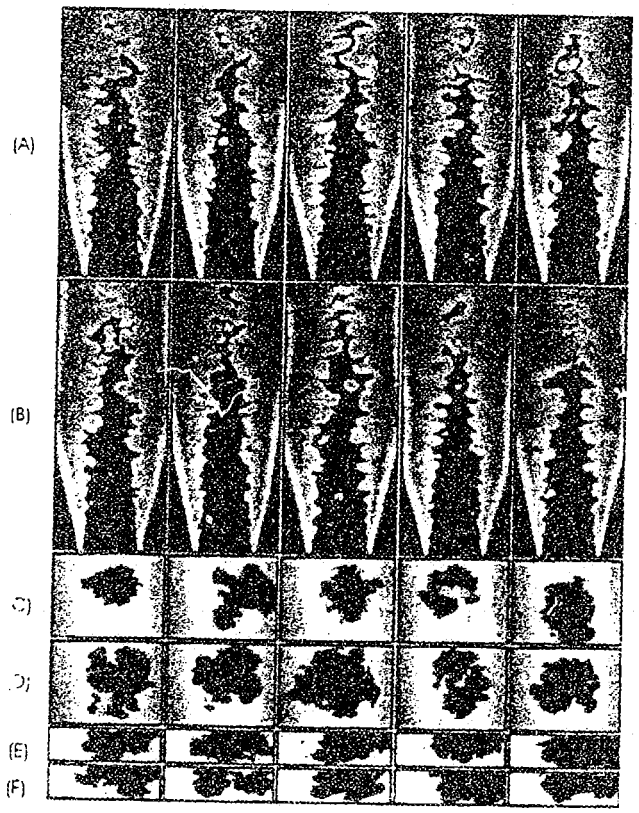

Figure 4. Flame images obtained by planar laser-induced fluorescence [36]: Rows (A) and (B) Bunsen-type burner. Rows (C) and (D): Horizontal cross-section in engine. Rows (E) and (F): Vertical cross-section in engine. The flame images were obtained using laser-induced fluorescence of biacetyl in the engine and of OH radicals in the Bunsen flame.Nondimensional turbulence intensities of the Bunsen and engine flames vary from 0.25 to 2.

SURFACE DENSITY OF FLAME FRONTS

The most common experimental technique of measuring the flame surface density is the use of the thin laser sheet tomography to mark the reaction boundary (or flame front location) between the unburned reactants and the products. The instantaneous flame fronts can be visualized either by laser induced fluorescence of OH or CH, or by Mie scattering from oil droplets that dissappear at the flame front. Obviously these methods give two-dimensional information whereas almost all turbulent flames are locally three-dimensional. It is also possible to deduce the flame surface density information using flame crossing times from Rayleigh scattering experiments.

Most of the experimental data on flame surface density are limited to low turbulence intensities, e.g. [36,56-58]. In most of studies, the three-dimensional information has been extracted from the two-dimensional data by making certain assumptions. In [36], images from orthogonal planes have been used to determine the mean orientation angle, and thus the directional cosine, along the line of intersection of the planes in a spark ignition engine. Several studies concluded that in a wide range of flame geometries, the mean flamelet direction cosine is about 0.65-0.75 [36,59,60]. Bingham et al. [61] extended this technique to crossed-plane tomography, for direct determination of the instantaneous flamelet surface normals by using data from tomographic images recorded simultaneously from two orthogonal laser illumination planes, which could be used to determine the flame surface density.

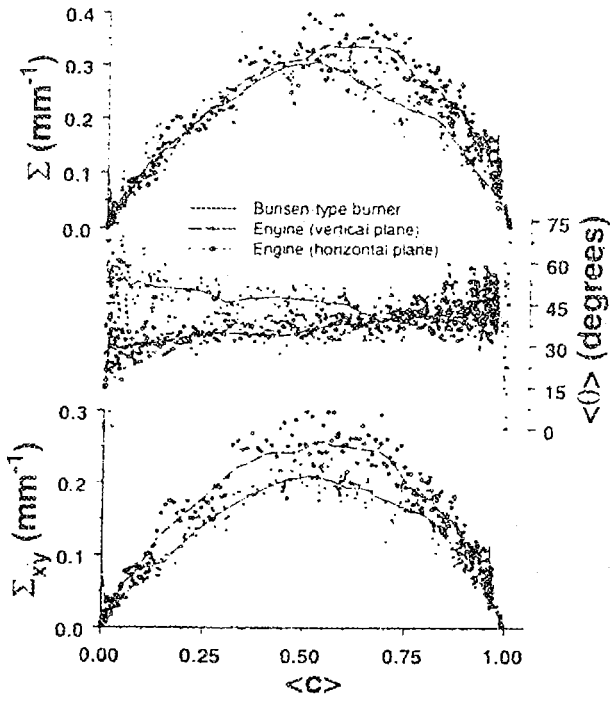

Figure 5. Mean length of flame front per unit area, Σ_{xy}, orientation angle, $< \theta >$, and flame surface density, Σ, as a function of mean progress variable $< c >$ measured on central axis of the Bunsen flames, and in the vertical plane of the engine, along the line of intersection with the horizontal plane. Lines are smoothed fits to the data points [36].

Experimental data obtained in Bunsen flames and firing homogenous charge spark ignition engines at low turbulence intensities, i.e., u'/S_L less than 2, did not show any significant variation of the flame surface density with turbulence intensity [36,64]. Typical flame front images obtained in a Bunsen-type burner and in a spark-ignition engine are shown in Fig.4. The engine used for obtaining the flame front images and the imaging method are described in [36]. Briefly, the combustion chamber of this spark-ignition engine provides optical access through four fused silica side windows and an extended piston with a fused silica top. The spark is located in the center of the chamber by extended electrodes. The engine has a bore and stroke of 86 and 82 mm, respectively, resulting in a displacement volume of 476 cm^3, and the compression ratio is 7.7. The Σ profiles reported in [36], including

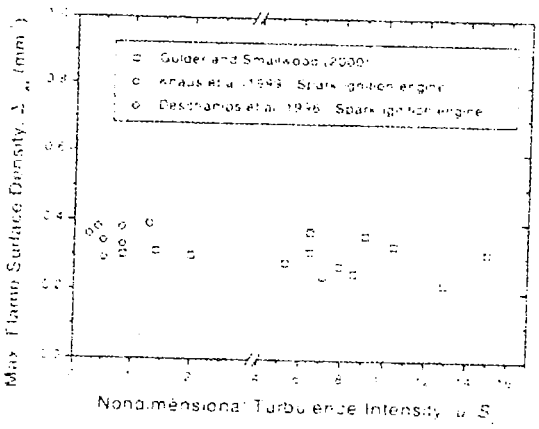

Figure 6. Maximum flame surface density versus nondimensional turbulence intensity [62,68]. Flame surface densities of engine flames are from [36] and [63].

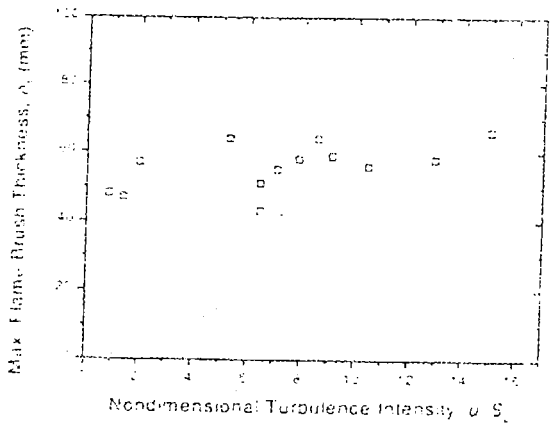

Figure 7. Variation of the turbulent flame brush thickness with nondimensional turbulence intensity, u'/S_L [62,68].

individual data points. for one Bunsen flame and one engine condition are shown on Fig.5 as a function of mean progress variable $< c >$. The mean two-dimensional flame surface density, Σ_{2D}, and the mean orientation angle, $< \theta >$, where $\cos(\theta) = n_y$, that produced the Σ profiles are also given in Fig.5.

Results from direct numerical simulation efforts [54] also did not show any dependence of the flame surface density on turbulent rms velocity. Recently, our research group has reported flame surface density measurements in turbulent premixed Bunsen flames covering the turbulence intensity range of u'/S_L from 0.9 to 15 [62]. An axisymmetric Bunsen-type burner with nozzle diameters of 11.2 mm and 22.4 mm produced the turbulent premixed conical flames studied in [62].

Σ_{max} had little variation over the range of u'/S_L (0.9 to 15.0) investigated in [62], as can be seen in Fig. 6. The data in Fig.6 also include two sets of results from spark-ignition engine measurements reported in [36] and [63]. Clearly, there is no relationship between flame surface density and turbulence intensity. It has been shown that $(\Sigma \cdot \Lambda)$ increases with increasing u'/S_L at low turbulence intensities [58]. However, this is likely due to the contribution from the integral length scale, which also varied in the reported experiments. In fact, there is some indication that the flame surface density may have an inverse relationship with the integral length scale [36,64], when normalized by the laminar flame thickness.

DISCUSSION OF SURFACE DENSITY RESULTS

In view of Eq.17, if we ignore the flame stretch and curvature effects for the sake of discussion, the turbulent burning velocity is affected by the volume-averaged flame surface density, $\overline{\Sigma}$, and the volume of the flame brush, V, i.e.,

$$S_T = S_L \frac{\overline{\Sigma} \cdot V}{A_o} \qquad (18)$$

However, as shown in Fig.6, experimental and numerical results indicate that over a large range of turbulence intensities, flame surface density is not sensitive to the turbulence intensity [36,54,56,62].

In Bunsen flames, the volume V enclosing the turbulent flame brush can be estimated, to a first approximation, to be proportional to the thickness of the turbulent flame brush at the tip of the flame along the burner centerline, i.e.,

$$V \approx \frac{1}{3}\pi r^2 \delta_T \qquad (19)$$

where r is the radius of the Bunsen burner and δ_T is the maximum flame brush thickness at the tip of the flame. Figure 7 shows the variation of the maximum flame brush thickness of the Bunsen flames with nondimensional turbulence intensity [62,68]. There is no apparent dependence of flame brush thickness on turbulence intensity. Deschamps [65] reported turbulent flame brush thickness measurements in Bunsen flames. Her results do not show any evidence of dependence of δ_T on either integral length scale or the turbulence intensity. In view of Eq.19, this implies that the volume V is not sensitive to turbulence parameters.

The observations that the flame surface density and the volume that encloses the mean reaction zone are not sensitive to the turbulence intensity have some serious implications. All of the experimental observations on turbulent premixed flames have shown that the turbulent burning velocity increases with increasing turbulence intensity. Thus the flame surface density and/or the volume that encloses the mean reaction zone, V, are expected to increase with increasing u'/S_L in accordance with Eq.17, however, neither of them show evidence of dependence on the flow turbulence. If the surface density is a true

measure of the characteristics of the wrinkled flame surface, then Eq.17 may not be a reasonable assumption for the flamelet regime, and the turbulent premixed combustion analysis and predictions should not be based only on the geometry of the flame front surface. These flame surface density results show that it would not be possible to describe the flame front propagation in spark-ignition engine combustion by the flame surface density approach, and the assumption that the turbulent flame front is a passive scalar surface can not be justified.

If the area increase (due to increasing turbulence) does not explain the increase in mean burning rate, then it may be proposed that the turbulent transfer of species and heat (enhanced by small scale turbulence) should have a significant role in turbulent premixed combustion. This observation supports the analytical work of Zimont [69] and Ronney and Yakhot [39]. Results obtained in [39] concludes that the effect of scales smaller than the laminar flame front thickness on turbulent transport are probably significant for most flames at sufficiently high turbulence intensities.

CONCLUDING REMARKS

The two approaches that are commonly used with the laminar flamelets assumption to estimate the increase in the wrinkled flame surface area, namely the fractal description of the turbulent premixed flame surfaces and the flame surface density concept have been reviewed in relation to the spark ignition engine combustion, and the formulations that link the flame surface density and the fractal characteristics to turbulent flame velocity have been summarized.

An evaluation and comparison of the experimental fractal characteristics data of turbulent premixed flames indicated, for nondimensional turbulence intensities up to 15, the mean fractal dimension is about 2.2 and it does not show any dependence on turbulence intensity. This value of the fractal dimension is much lower than the values found by several other studies that showed that the fractal dimension asymptotically reaches to 2.35 – 2.37 when the nondimensional turbulence intensity u'/S_L exceeds 3.

The fractal parameters obtained so far, reported in the combustion literature, are not capable of correctly predicting the turbulent burning velocity. If the fractal geometry approach is yielding a true measure of the wrinkled flame surface area, then our assessment casts doubt on the assumption that the nondimensional turbulent burning velocity can be estimated from the ratio of the wrinkled flame surface area to the flow cross section, and give credence to models which assign significance to increased transfer of species and heat (enhanced by small scale turbulence), in addition to the flame surface area increase. On the other hand, the fractal area expression currently in use may require modification to give a better estimate of the flame front area.

An examination of the experimental and numerical flame surface density data and the volume that encloses the mean reaction zone (flame brush volume) indicated that these two variables are independent of the nondimensional turbulence intensity. If the surface density is a true measure of the characteristics of the wrinkled flame surface, then Eq.14 may not be valid for the flamelet regime, and the turbulent premixed combustion analysis and predictions for spark ignition engine combustion should not be based only on the geometry of the flame front surfaces. The assumption made in fractal and surface density approaches that the turbulent flame front is a passive scalar surface can not be justified.

ACKNOWLEDGMENTS

We acknowledge the invaluable contributions of our colleagues, D. R. Snelling, B. M. Deschamps and R. Smith. This work was partially supported by the Canadian Government's PERD Program (Project No. 15113).

CONTACT

The authors are with the National Research Council of Canada, ICPET, Combustion Research Laboratory, Bldg. M-9, 1200 Montreal Road, Ottawa, Ontario K1A 0R6, Canada. The E-mail addresses are:
omer.gulder@nrc.ca
greg.smallwood@nrc.ca.

REFERENCES

1. Daneshyar, H., and Hill, P. G., *Progress in Energy and Combustion Science*, 17, pp.47-73, 1987.

2. Semenov, E. S., "Studies of Turbulent Gas Flow in Piston Engines", NACA Technical Translation, F-97, 1963.

3. Bracco, F. V., *Combustion Science and Technology*, 58, pp. 209 - 230, 1988.

4. Smith, J. R., SAE Paper No. 820043.

5. Keck, J. C., *Nineteen Symposium (Int.) on Combustion*, The Combustion Institute, Pittsburgh, PA, pp. 1451-1466, 1987.

6. Abraham, J., Williams, F. A., and Bracco, F. V., SAE Paper No. 850345.

7. Damköhler, G., *Ze. Elektroch. 46:601-652(1940)*. (English Translation NACA TM 1112, 1947.)

8. Williams, F. A., *Combustion Theory* (2nd ed) Benjamin / Cummings, Menlo Park, California, 1985, Ch.10.

9. Bray, K. N. C., in *Turbulent Reacting Flows* (Ed. P. A. Libby, F. A. Williams), Springer-Verlag, 1980, p.115.

10. Borghi, R., in *Recent Advances in the Aerospace Science* (Ed. C. Casci), Plenum, 1985, p.117.

11. Abdel-Gayed, R. G., Bradley, D., and Lawes, M., *Proceedings of Royal Society London* A 414:389-413 (1987).

12. Peters, N., *Twenty-First Symposium (Int.) on Combustion*,

The Combustion Institute, Pittsburgh, PA. 1986. pp.1231-1250.

13. Gülder, Ö. L., *Twenty-Third Symposium (Int.) on Combustion*, The Combustion Institute, Pittsburgh, PA, 1990, pp.743-750.

14. Lipatnikov, A. N., and Chomiak, J., SAE Paper No. 972993.

15. Bray, K. N. C., in *Complex Chemical Reactive Systems* (J. Warnatz and W. Jäger, Eds.), Springer-Verlag, 1987, pp 356 - 375.

16. Cant, R. S., and Bray, K. N. C., *Twenty-Second Symposium (Int.) on Combustion*, The Combustion Institute, Pittsburgh, PA, 1987, pp.791-799.

17. Bray, K. N. C., and Cant, R. S., *Proceedings of Royal Society London* A 434:217-240 (1991).

18. Poinsot, T., Veynant, D., and Candel, S., *Twenty-Third Symposium (Int.) on Combustion*, The Combustion Institute, Pittsburgh, 1990, pp.613-619.

19. Roberts, W. L., Driscoll, J. F., Drake, M. C., and Goss, L. P., *Combustion and Flame* 94:58-69 (1993).

20. Bedat, B., and Cheng, R. K., *Combustion and Flame*, 100: 485-494, 1995.

21. Peters, N., *Journal of Fluid Mechanics*, 384:107-132 (1999).

22. Chin, Y. W., Mathews, R. D., Nichols, S. P., *Proceedings of the Second COMODIA 90*, JSME, 1990, pp. 81-86.

23. Wirth, M., Keller, P., and Peters, N., SAE Paper No. 932646, 1993.

24. Delhaye, B., and Cousyn, B., SAE Paper No. 961960, 1996.

25. Boudier, P., Henriot, S., Poinsot, T., and Baritaud, T., *Twenty-Fourth Symposium (International) on Combustion*, The Combustion Institute, Pittsburgh, 1993, pp. 503-510.

26. Zhao, X., Matthews, R. D., and Ellzey, J. L., *Proceedings of the Third COMODIA 94*, JSME, 1994, pp. 157-162.

27. Mandelbrot, B. B., *The Fractal Geometry of Nature*, Freeman, New York, 1983, Ch.12.

28. Gouldin, F. C., *Combustion and Flame* 68:249-266 (1987).

29. Gülder, Ö. L., *Twenty-Third Symposium (Int.) on Combustion*, The Combustion Institute, Pittsburgh, 1991, pp.835-842.

30. Gouldin, F. C., Bray, K. N. C., and Chen, J.-C., *Combustion and Flame* 77:241-259 (1989).

31. Gouldin, F. C., and Miles, P. C., *Combustion and Flame* 100:202-210 (1995).

32. Gouldin, F. C., *A Refined Fractal Based Model for Mean Rate of Product Formation in Turbulent Flames* presented at the Joint Meeting of the Central States, Western States, and Mexican National Sections of the Combustion Institute, San Antonio, Texas, April 23-26, 1995.

33. Kerstein, A. R., *Combustion Science and Technology* 60: 441-445(1988).

34. Lee, T.-W., Lee, J. G., Nye, D. A., and Santavicca, D. A., *Combustion and Flame* 94:146-160 (1993).

35. Smallwood,G.J., Gulder, O. L.,Snelling,D.R., Deschamps, B. M., and Gökalp, I., *Combustion and Flame* 101:461-470 (1995).

36. Deschamps, B. M., Smallwood, G. J., Prieur, J., Snelling, D. R., and Gülder, O. L., *Twenty-Sixth Symposium (Int.) on Combustion*, The Combustion Institute, Pittsburgh, PA, 1996, pp.613-619.

37. Mantzaras, J., Felton, P. G., and Bracco, F. V., SAE Paper No. 881635,1988.

38. Mantzaras, J., Felton, P. G., and Bracco, F. V., *Combustion and Flame* 77:295-310 (1989).

39. Yoshiyama, S., Hamamoto, Y., Tomita, E., and Zhong, Z., *The Forth International Symposium COMODIA*, 1988, pp. 209-214.

40. Murayama, M., and Takeno, T., *Twenty-Second Symposium (Int.) on Combustion*, The Combustion Institute, Pittsburgh, 1989, pp.551-559.

41. North, G. L., and Santavicca, D. A., *Combustion Science and Technology* 72:215-232 (1990).

42. Yoshida, A., Kasahara, M., Tsuji, H., and Yanagisawa, T., *Combustion Science and Technology* 103:207-218 (1994).

43. Das, A. K., and Evans, R. L., *Experiments in Fluids* 22:312-320 (1997).

44. Gülder, Ö. L., Smallwood, G. J., Wong, R., Snelling, D. R., Smith, R., Deschamps, B. M., and Sautet, J.-C., *Combustion and Flame*, 120: 407-416, 2000.

45. Ronney, P. D., and Yakhot, V., *Combustion Science and Technology* 86:31-43(1992).

46. Mantzaras, J., *Combustion Science and Technology* 86:135-162(1992).

47. Clavin, P., *Progress in Energy Combustion Science* 11:1-59(1985).

48. Choi, C. R., and Huh, K. Y., *Combustion and Flame*, 114, 336-348(1998).

49. Bray, K. N. C., Libby, P. A., and Moss, J. B., *Combustion Science and Technology* 41:143-172 (1984).

50. Bray, K. N. C., Champion, M., and Libby, P. A., in *Turbulent Reacting Flows* (Ed. P. A. Libby, F. A. Williams), Springer-Verlag, 1980, p.40.

51. Pope, S. B., *International Journal of Engineering Science* 26:445-469 (1988).

52. Trouvé, A., and Poinsot, T., *Journal of Fluid Mechanics* 278: 1-31 (1994).

53. Marble, F. E., and Broadwell, J. E., "The Coherent Flame

Model for Turbulent Chemical Reactions." Project Squid. Technical Report TRW-9-PU. January,1977.

54. Boger, M., Veynante, D., Boughanem, H., and Trouvé, A., *Twenty-Seventh Symposium (Int.) on Combustion*, The Combustion Institute, Pittsburgh, 1998, pp 917-925.

55. Prasad, R. O. S., Paul, R. N., Sivathanu, Y. R., and Gore, J. P., *Combustion and Flame* 117:514-528 (1999).

56. Deschamps, B., Boukhalfa, A., Chauveau,C., Gökalp, I. Shepherd, I. G., and Cheng, R. K., *Twenty-Fourth Symposium (Int.) on Combustion*, The Combustion Institute, Pittsburgh, 1992, pp.469-475.

57. Shepherd, I. G., *Twenty-Sixth Symposium (Int.) on Combustion*, The Combustion Institute, Pittsburgh, 1996, pp.373-379.

58. Ghenai, C., Chauveau, C., and Gökalp, I., *Twenty-Sixth Symposium (Int.) on Combustion*, The Combustion Institute, Pittsburgh, 1996, pp.331-337.

59. Shepherd, I. G., and Ashurst, W. T., *Twenty-Forth Symposium (Int.) on Combustion*, The Combustion Institute, Pittsburgh, 1992, pp.485-491.

60. Zhang, Y., Bray, K. N. C., and Rogg, B., *Combustion Science and Technology* 137:347-358(1998)

61. Bingham, D. C., Gouldin, F. C., and Knaus, D. A., *Twenty-Seventh Symposium (Int.) on Combustion*, The Combustion Institute, Pittsburgh, 1998, pp.77-84.

62. Smallwood, G. J., Snelling, D. R., and Gülder, O. L., *17th ICDERS*, July 25-30, 1999, Heidelberg, Germany.

63. Knaus, D., Gouldin, F. C., Hinze, P. C., and Miles, P. C., SAE Paper No. 1999-01-3543, 1999.

64. Smallwood, G. J., and Deschamps, B. M., SAE Paper No. 962088, 1996.

65. Deschamps, B. M., "Etude Spatiale et Temporelle de la Structure Dynamique et Scalaire des Flammes Turbulentes Prémélangées de Methane-Air", Universite d'Orléans, Ph. D. Thesis, 1991.

66. Takeno, T., Murayama, M., and Tanida, Y., *Experiments in Fluids* 10:61-70(1990).

67. Üngüt, A., Gorgeon, A., and Gökalp, I., *Combustion Science and Technology* 92:265-290(1993).

68. Gülder, Ö. L., *Proc. Mediterranean Combustion Symposium*, Istituto di Ricerche sulla Combustione-CNR, Napoli, Italy 1999, pp.130-154.

69. Zimont, V. L., *Combustion, Explosion and Shock Waves* 15: 305-311(1979).